



# Why large porphyry Cu deposits like high Sr/Y magmas?

SUBJECT AREAS:

PETROLOGY

EARTH SCIENCES

GEOCHEMISTRY

MINERALOGY

Massimo Chiaradia<sup>1</sup>, Alexey Ulianov<sup>2</sup>, Kalin Kouzmanov<sup>1</sup> & Bernardo Beate<sup>3</sup>

<sup>1</sup>Section of Earth and Environmental Sciences, University of Geneva, 1205 Geneva, Switzerland, <sup>2</sup>Institute of Mineralogy and Geochemistry, University of Lausanne, 1015 Lausanne, Switzerland, <sup>3</sup>Escuela Politécnica Nacional, Dep.to de Geología, Ladrón de Guevara E11-253, Quito, Ecuador.

Received  
19 March 2012

Accepted  
10 September 2012

Published  
24 September 2012

Correspondence and  
requests for materials  
should be addressed to  
M.C. (Massimo.  
Chiaradia@unige.ch)

Porphyry systems supply most copper and significant gold to our economy. Recent studies indicate that they are frequently associated with high Sr/Y magmatic rocks, but the meaning of this association remains elusive. Understanding the association between high Sr/Y magmatic rocks and porphyry-type deposits is essential to develop genetic models that can be used for exploration purposes. Here we present results on a Pleistocene volcano of Ecuador that highlight the behaviour of copper in magmas with variable (but generally high) Sr/Y values. We provide indirect evidence for Cu partitioning into a fluid phase exsolved at depths of ~15 km from high Sr/Y (>70) andesitic magmas before sulphide saturation. This lends support to the hypothesis that large amounts of Cu- and S-bearing fluids can be accumulated into and released from a long-lived high Sr/Y deep andesitic reservoir to a shallower magmatic-hydrothermal system with the potential of generating large porphyry-type deposits.

Three-quarters of the world's Cu and one-fifth of the world's Au are currently supplied by porphyry systems<sup>1</sup>. It has been recognized for some time that porphyry-type deposits are associated with magmatic arcs<sup>2</sup>, but only in recent years have links with high Sr/Y (>40) andesitic to dacitic magmas been established<sup>3–10</sup>. The genesis of high Sr/Y arc magmas is a subject of debate, with interpretations for their origins including: (i) slab melting<sup>11,12</sup>, (ii) lower crust melting<sup>13,14</sup> or (iii) fractional crystallization of amphibole ± garnet<sup>15–18</sup>, possibly accompanied by crustal melting and assimilation<sup>19,20</sup>. On the other hand, there is growing evidence suggesting that the high Sr/Y magmas associated with porphyry systems are not slab melts<sup>21</sup>, but derive from magmatic evolution at mid- to deep crustal levels<sup>7–10,22,23</sup>. Here, magmas fractionate amphibole ± garnet but not plagioclase, leading to relative Y depletion and Sr enrichment in the residual melt. Fractional crystallization is often accompanied also by partial melting and assimilation of mid- to lower crustal rocks by the evolving magmas<sup>8</sup>.

The reasons of the association of porphyry-type deposits with high Sr/Y magmatic rocks remain speculative, although high water (>4 wt.%<sup>10</sup>) and sulphur (>1000 ppm<sup>24</sup>) contents as well as high oxidation states (>FMQ + 1.3–2, e.g.<sup>21,25</sup>) are intuitively critical factors<sup>7,8,10,22</sup>. Additionally, it is debated whether Cu is transferred to ore fluids directly from the magma<sup>26–28</sup> or through the intermediate formation of magmatic sulphides<sup>29–31</sup>. These processes may however occur independently in different porphyry systems.

Here we explore the association of high Sr/Y magmas with porphyry systems by investigating the behaviour of Cu in oxidized hydrous basaltic andesites of the Pleistocene Pilavo volcano (Western Cordillera of Ecuador). We provide indirect evidence that copper is exsolved into a fluid phase from a high Sr/Y andesitic magma at depths of up to ~15 km. This allows us to link into a coherent model two aspects that previous studies have considered to be critical in the formation of porphyry systems: (i) the role of deep mafic/intermediate intrusions recharging shallower felsic systems with fluids and metals<sup>32–36</sup>, and (ii) the role of water-rich high Sr/Y magmas<sup>9,22</sup>.

Pilavo magmas evolved initially at the mantle-crust boundary through fractionation of olivine and clinopyroxene<sup>37</sup>. This led to the formation of hydrous, high-alumina basaltic andesite melts with high Sr (>700 ppm), relatively high Sr/Y (~40) and very low Ni (<15 ppm)<sup>37</sup> concentrations. Subsequently these melts ascended up to mid-crustal levels where they underwent varying degrees of magmatic evolution in a composite reservoir. This evolution occurred through pronounced amphibole and clinopyroxene fractionation, crustal assimilation and incremental recharge by high-alumina basalts rising from depth<sup>37</sup>. This mid-crustal open system evolution, highlighted by the correlations between whole rock geochemistry (including Sr/Y), radiogenic isotopes and modal mineralogy, is remarkably similar to that of giant porphyry systems like Yanacocha<sup>8</sup> (Supplementary

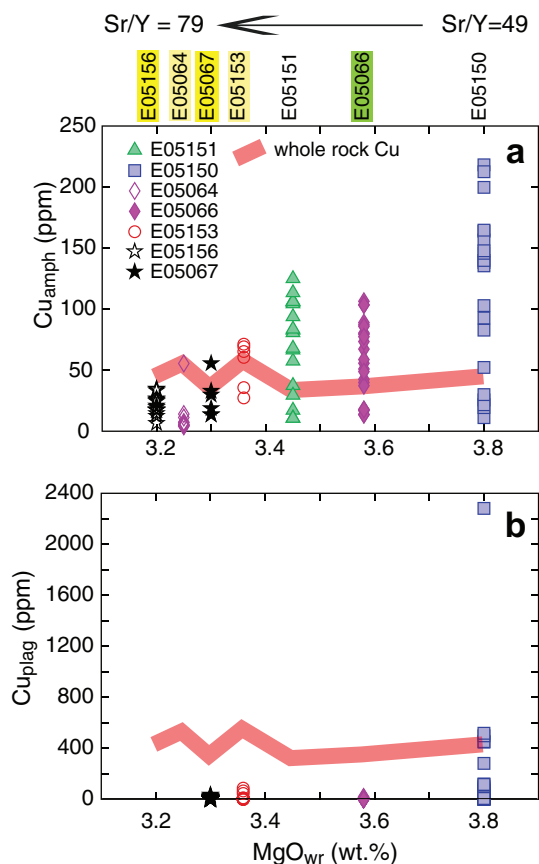


**Figure 1** | Maximum Cu concentrations in amphiboles (a) and plagioclases (b) decrease with increasing evolution (lower MgO, higher Sr/Y) of the host whole rocks. Cu-Fe-sulphides appear as inclusions in magnetite only in the more evolved rocks, colour-coded on the upper part of the diagram: green = very few sulphides (<10% of magnetite grains host sulphides); light yellow = medium number of sulphides (10–30%); yellow = abundant sulphides (>30%).

Material 1). Therefore, the Pilavo magmatic system is suitable for the investigation of magmatic processes potentially associated with the development of porphyry systems.

Basaltic andesites of Pilavo are characterized by variable contents of incompatible elements (e.g., Th, U, Zr, REE, Sr, Ba) and Sr/Y values (40 to 80), which are a result of contrasting residence times in the mid-crustal reservoir<sup>37</sup>. Incompatible element poorer magmas with lower Sr/Y (40–50) did not evolve significantly in the mid-crustal reservoir and reflect the compositions of the hydrous, high-alumina basaltic andesites formed at the mantle-crust boundary<sup>37</sup>. These magmas crystallized small amounts of amphibole (<3% modal) during ascent to shallow levels where degassing caused extensive plagioclase crystallization, magma stalling, and mixing in the conduit (at  $P < 0.1$  GPa) with high-alumina basaltic magmas coming from depth<sup>37</sup>. In contrast, incompatible element-rich magmas with higher Sr/Y (>50 and up to 80) resulted from more or less prolonged evolution in the mid-crustal (~0.4 GPa) composite reservoir where they fractionated, assimilated and were recharged by the high-alumina mafic magma<sup>37</sup>. Magmas with higher Sr/Y values contain significantly more amphibole (up to ~20% modal)<sup>37</sup>. Therefore, modal amphibole concentrations suggest that increasing water contents in magmas with higher Sr/Y values occur as a consequence of more extensive fractionation at mid-crustal levels<sup>37</sup>. Throughout the series, magmas are strongly oxidized ( $fO_2 = NNO + 1.5$  to  $+3.3$ ). The high oxidation state of the Pilavo magmas is recorded by magnetite-ilmenite pairs within amphibole and is likely the result of both an oxidized mantle source and an intracrustal evolution in which amphibole fractionation occurs<sup>37</sup>.

## Results

We have analysed Cu contents in plagioclase, amphibole and clinopyroxene phenocrysts by LA-ICPMS (see Methods and Supplementary Material 2). Maximum  $Cu_{\text{pyroxene}}$  contents remain consistently below 30 ppm throughout the Pilavo series rocks (Supplementary Material 2). In contrast, maximum  $Cu_{\text{amphibole}}$  and  $Cu_{\text{plagioclase}}$  contents vary with rock geochemistry (Figure 1): rocks with lower Sr/Y values have much higher  $Cu_{\text{amphibole}}$  (>200 ppm) and  $Cu_{\text{plagioclase}}$  (generally 400–500 but up to >2000 ppm) than rocks with high Sr/Y ( $Cu_{\text{plagioclase}}$  and  $Cu_{\text{amphibole}} = 40–50$  ppm). In low Sr/Y rocks the highest  $Cu_{\text{plagioclase}}$  contents occur in plagioclase growth zones with abundant fluid and melt inclusions, situated between core and rim (Figures 2a–b). Within the inclusion-free zones the  $Cu_{\text{plagioclase}}$  contents drop significantly (<5 ppm; Supplementary Materials 2 and 5). During ablation,  $Cu_{\text{amphibole}}$  exhibits a smooth and stable intensity signal (Supplementary Material 3). In contrast, the  $Cu_{\text{plagioclase}}$  intensities resulting from the ablation of the inclusion-rich areas of plagioclase vary erratically with high peaks lifting the average concentrations of the time-integrated analyses (Supplementary Material 3). These peaks are likely the result of ablating Cu-rich inclusions within the plagioclase. In order to test such a hypothesis we have investigated by SEM plagioclase fragments that had been hammer-broken and not washed to preserve the integrity of soluble phases possibly occurring in fluid inclusions. Indeed, SEM imaging reveals tiny ( $\leq 1 \mu\text{m}$ ) Cu-Fe-sulphides within  $\mu\text{m}$  to sub- $\mu\text{m}$  sized fluid inclusions, which are too small to be individually analysed by LA-ICPMS (Figures 2c–f and Supplementary Material 4). These are the most likely candidates for the Cu peaks observed within the LA-ICPMS analyses of plagioclases. Apart from the Cu-Fe sulphide phases no other mineral phases are visible in these “empty” inclusions. Additionally, we did not observe salt deposits within and/or around the broken inclusions, which would have formed by sudden evaporation of a saline fluid at the moment of the hammer-induced opening of the inclusions (Figures 2b–c and Supplementary Material 4). We consider this as an indirect evidence for a low-salinity, vapour-rich nature of the fluid of these inclusions. Only in one case we observed a possible salt deposit around a broken fluid inclusion containing a Cu-Fe-sulphide (Figure b of Supplementary Material 4). This might suggest the occurrence also of some saline fluid inclusions.

In Pilavo rocks plagioclase occurs dominantly as micro-phenocrysts in the groundmass, suggesting that it has crystallized during decompression at shallow levels. This is supported by a decrease in the anorthite content from the inclusion-rich cores ( $An \geq 80$  mol.%) to the inclusion-free rims ( $An \leq 70$  mol.%). Such an anorthite change is consistent with a decrease in the water content of the magma coexisting with plagioclase<sup>37,38</sup>. Thus, the melt/fluid inclusion-rich zones document plagioclase growth during decompression-induced degassing. During degassing Cu, as experimentally predicted<sup>39–41</sup>, has partitioned into the vapour-rich fluid phase, which was trapped within the plagioclase-hosted fluid inclusions. Cu-sulphides have subsequently precipitated from such vapour-rich fluid phase within the inclusions.

The systematically decreasing  $Cu_{\text{amphibole}}$  concentrations in rocks with increasing Sr/Y values and decreasing MgO (Figure 1a) cannot reflect magmatic fractionation of Cu-bearing minerals. Sulphides, which can incorporate large amounts of  $Cu^{42}$ , are clearly late-stage in both lower (see above) and higher Sr/Y rocks (see below). The Cu partition coefficient between melt and a clinopyroxene-amphibole assemblage fractionating in Pilavo magmas with a conservative ratio of  $1:1$ <sup>37</sup> is  $>1$ . Therefore, Cu concentrations would increase in the residual melt during fractionation of such an assemblage (amphibole and clinopyroxene partition coefficient values from<sup>43</sup> and <http://earthref.org/GERM/>, respectively). This is supported by: (i) the core-to-rim increase of  $Cu_{\text{amphibole}}$  concentrations in amphiboles of lower Sr/Y rocks, (ii) the core-to-rim decreases in compatible

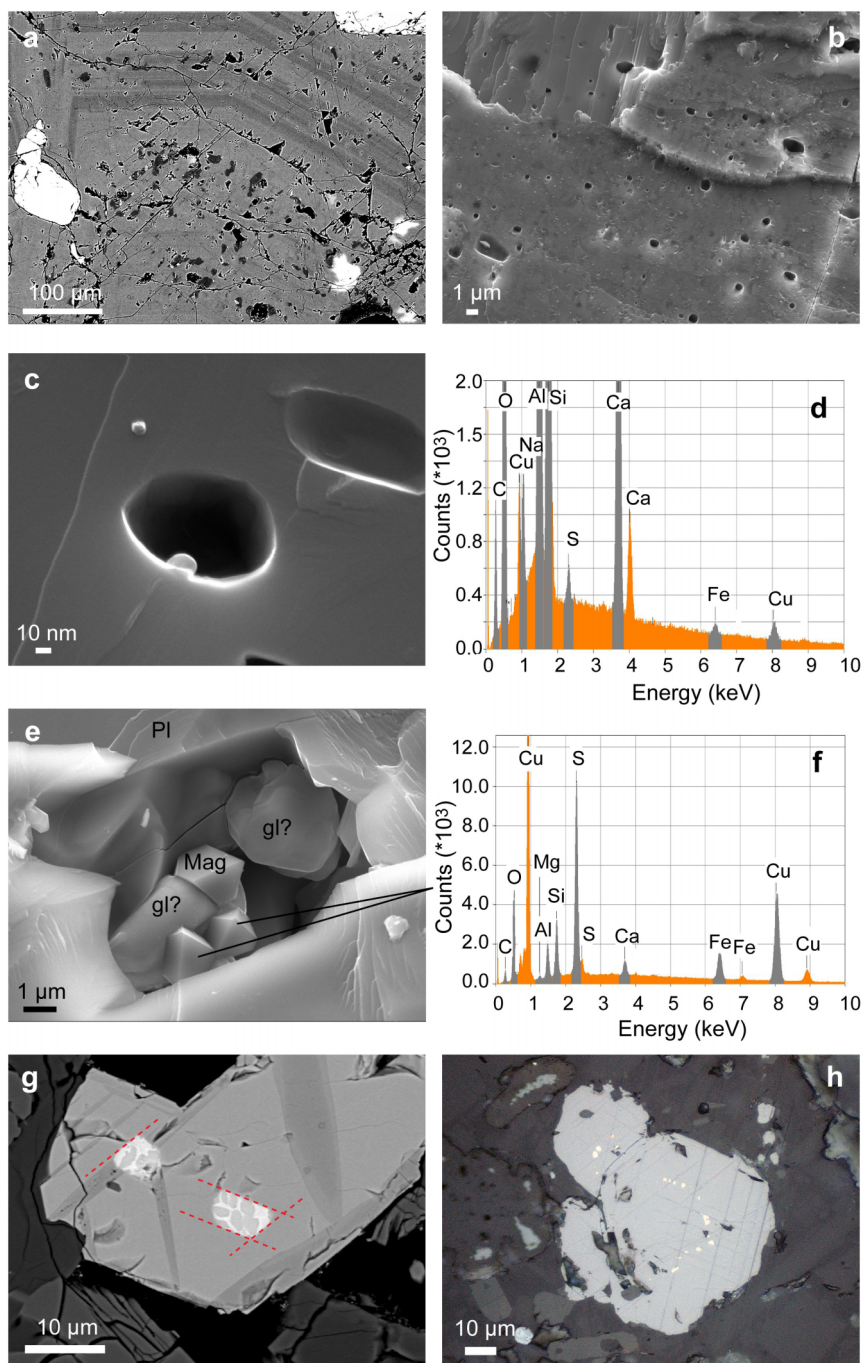


**Figure 2** | SE images (a–c, e) and EDS spectra (d, f) of unwashed and unpolished hammer-broken fragments of basaltic andesite (sample E05150). The images show fluid/melt inclusion-rich zones within plagioclase phenocrysts (a) with abundant empty fluid inclusions (b) and the occurrence of Cu-Fe-sulphides within some of them (c–d). The most common occurrence of Cu-Fe-sulphides is that of Figure 2c (see Supplementary Material 4 for additional pictures). Apart from the Cu-Fe-sulphide phase (c) no other mineral phases are visible in these inclusions. Additionally within and around the inclusions we never observed salt deposits that might have formed upon hammer-induced rupture of the fluid inclusions if these contained saline fluids. This suggests that the inclusions are low-salinity, essentially vapour-rich. In one case (e–f) we observed the occurrence of a crystalline (pseudo-)octahedral Cu-(Fe-)sulphide in association with magnetite in a fluid inclusion perhaps associated with melt (gl?). (g) BSE image of groundmass magnetite with ilmenite exsolutions along crystallographic planes and Cu-Fe-sulphide inclusions displaying quenched textures consisting of rounded blebs of a Cu-poor phase (10–20 wt.% Cu; dark grey) inside a Cu-richer (30–40 wt.% Cu; bright) host (EDS analyses: Supplementary Material 9 and 10). The shapes of the inclusions are often delimited by crystallographic planes (dashed red lines), parallel to the ilmenite exsolutions (sample E05067). Groundmass magnetite hosting a swarm of Cu-Fe-sulphide inclusions (h) parallel to growing crystal surfaces (?) (reflected light, parallel nicols: sample E05156). Abbreviations: Pl = plagioclase; Mag = magnetite; gl = glass.

elements (Mg, Ni) and (iii) the core-to-rim increases in incompatible elements (e.g., Zr, La, Hf) (Supplementary Material 6). Such zoning highlights the incompatible behaviour of Cu during magmatic differentiation under oxidized conditions<sup>44</sup>. We have modelled the

increase of Cu concentrations in Pilavo magmas that would result from their evolution through the recharge, assimilation, fractional crystallization (RAFC) process proposed by<sup>37</sup>. Modelling is based on 5 steps of RAFC (Supplementary Material 7) for a mildly incompatible

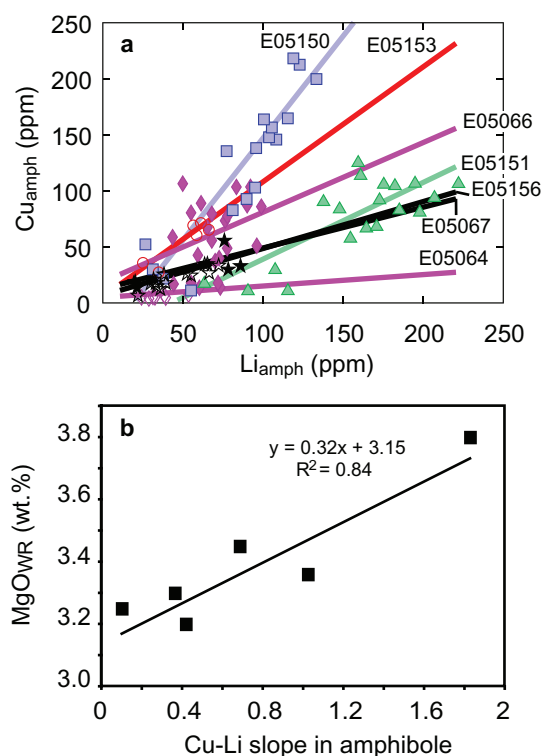


**Figure 3 | Correlations between Cu and Li contents of amphiboles in Pilavo andesites.** (a) Cu and Li contents of amphiboles ( $Cu_{ambph}$ ,  $Li_{ambph}$ ) correlate within each whole rock sample (except E05066) following linear trends with different slopes: E05150,  $Cu = 1.83 * Li - 39.21$ ,  $R = 0.91$ ; E05153,  $Cu = 1.03 * Li + 3.15$ ,  $R = 0.91$ ; E05066,  $Cu = 0.62 * Li + 15.75$ ,  $R = 0.32$ ; E05151,  $Cu = 0.69 * Li - 32.93$ ,  $R = 0.79$ ; E05156,  $Cu = 0.42 * Li + 3.61$ ,  $R = 0.87$ ; E05067,  $Cu = 0.37 * Li + 9.62$ ,  $R = 0.73$ ; E05064,  $Cu = 0.10 * Li + 1.96$ ,  $R = 0.78$ . (b) Cu-Li slopes defined by amphibole populations of each different whole rock sample (Figure 3a) correlate with evolution indices of the whole rock (e.g., MgO). Sample E05066 has not been plotted because of the poor correlation coefficient defined by its amphiboles in the Cu-Li space (Figure 3a).

behaviour of Cu ( $K_{melt/bulk\ minerals} = 2$ ). The calculated Cu concentrations for the most evolved Pilavo magma with the highest ( $\sim 80$ ) Sr/Y value of Pilavo rocks would be  $\sim 100$  ppm. This is significantly higher than the measured Cu concentrations (37–58 ppm) in whole rocks with similarly high Sr/Y values (70–80).

An alternative which can explain the decreasing  $Cu_{amphibole}$  concentrations in the rocks with higher Sr/Y values is that amphibole has crystallized from or has equilibrated with magmas that have previously exsolved a fluid phase (see also<sup>33,45</sup>). In fact, Cu will partition into the fluid phase upon fluid saturation of a magma ( $K_{fluid/melt} > 1$  for Cu<sup>39–41</sup>) and the magma coexisting with such a fluid will consequently become Cu-poorer. Although recent work by<sup>46</sup> suggests relatively low volatile phase/mafic melt partition coefficients of 2–6 for Cu, these values were calculated for an anhydrous basaltic melt. The water-rich Pilavo basaltic andesite magmas share little resemblance to anhydrous magmas and clearly additional work is needed<sup>46</sup> to quantify Cu partitioning into a fluid phase exsolved from hydrous andesitic magmas. Amphiboles crystallized at  $P \sim 0.4$  GPa in the more evolved (higher Sr/Y) rocks of Pilavo<sup>37</sup>. Therefore, fluid saturation and the associated Cu partitioning into such fluid phase must have occurred at relatively deep crustal levels (up to  $\sim 15$  km).

$Cu_{amphibole}$  contents correlate significantly with  $Li_{amphibole}$  contents within each sample (Figure 3a; see also<sup>43</sup>). Like Cu, also Li has a  $K_{fluid/melt} > 1$ <sup>47</sup> but  $K_{amphibole/fluid}$  for Li/Cu is  $> 1$ <sup>43,48</sup>, i.e., Li has less affinity for the fluid phase compared to Cu. Therefore,

systematically shallower slopes of Cu-Li correlations in amphiboles of increasingly evolved (higher Sr/Y) rocks (Figure 3b) further support amphibole crystallization from or equilibration with magmas that have increasingly exsolved a fluid phase. Diffusive equilibration of Cu in amphibole, potentially explaining the low Cu and flat core-to-rim Cu profiles of amphiboles from higher Sr/Y rocks (Supplementary Material 6), would require only a few years of magmatic residence time (Supplementary Material 8). That in higher Sr/Y rocks most of the Cu has partitioned into the fluid phase at high pressure is further confirmed by the very low Cu contents in the fluid/melt inclusion-rich zones of their plagioclase phenocrysts compared to the fluid/melt inclusion-rich zones of plagioclase in lower Sr/Y rocks (Supplementary Material 5). In other words, in contrast with lower Sr/Y magmas there was little Cu left in the higher Sr/Y magmas during shallow level decompression-driven fluid exsolution when plagioclase phenocrysts crystallized.

Higher Sr/Y rocks have similar whole rock Cu contents (37–58 ppm) to lower Sr/Y rocks (32–64 ppm). However, our modelling (see above and Supplementary Material 7) indicates that the most evolved magmas (with higher Sr/Y values) should contain higher Cu concentrations ( $\sim 100$  ppm) than those actually measured in the similarly evolved whole rocks ( $< 60$  ppm). From this we infer that a portion of the Cu has escaped from the Cu-rich and high Sr/Y andesitic magma along with the fluid phase. Cu is hosted by different mineral phases in the two rock types. In higher Sr/Y rocks the bulk of Cu is hosted by abundant, several  $\mu m$ -sized, Cu-Fe-sulphides occurring within groundmass magnetite (Figure 2e–f; Supplementary Material 9). In lower Sr/Y rocks such large Cu-Fe sulphides associated with magnetite have not been observed and the bulk of Cu occurs in the tiny ( $\leq 1 \mu m$ ) Cu-sulphides within plagioclase-hosted fluid inclusions (Figure 2c) and in Cu-rich amphiboles. The exclusive association of Cu-sulphides with magnetite in high Sr/Y rocks highlights the important role of magnetite crystallization in causing sulphide saturation in silicate magmas<sup>44,49</sup>. Following<sup>44</sup>, sulphide saturation might have occurred within the melt boundary layer surrounding growing magnetite due to a rapid switch in sulphur redox conditions, which was triggered by magnetite crystallization. Based on textural observations<sup>37</sup>, the groundmass magnetite of high Sr/Y rocks crystallized late, after amphibole and synchronous with plagioclase and clinopyroxene microcrysts. These observations are in agreement with the crystallization sequence of hydrous andesite at  $P > 0.2$  GPa<sup>50</sup> (Figure 4). The association of Cu-Fe-sulphides with late-stage magnetite indicates that magnetite-induced sulphide saturation of the magma occurred after the high pressure Cu partitioning into the fluid phase. A partial fluid-to-sulphide melt transfer of Cu and S from the fluid phase into the sulphide melt formed in the boundary layer around magnetite crystals could have been prompted by the preferential aggregation of fluid bubbles to crystallising magnetite<sup>51</sup>. Alternatively, Cu hosted by Cu-sulphides could have been derived from the residual Cu present in the melt after fluid partitioning at high pressure.

## Discussion

Porphyry systems result from a complex combination of magmatic, hydrothermal and tectonic factors<sup>52</sup> and, despite common general features, significant differences exist among them. In this work we explore the reasons why several major porphyry systems are spatially and temporally associated with high Sr/Y magmas. Nonetheless, we would like to emphasize that not all porphyry systems have an apparent association with high Sr/Y magmas and that alternative interpretations, differing more or less significantly from our, have been proposed for the association of porphyry-type deposits with high Sr/Y magmas<sup>3,7,9,10,21</sup>.

Our results provide indirect evidence that Cu partitions into a fluid phase before sulphide saturation at both shallow ( $\sim 0.1$  GPa) and relatively deep (up to  $\sim 0.4$  GPa) crustal levels. Analyses of coexisting

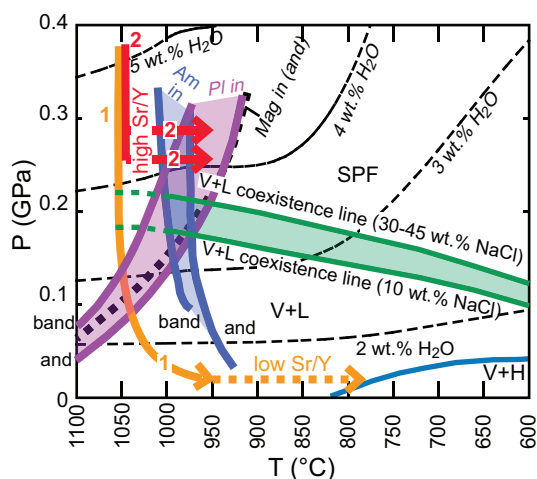


**Figure 4** | P-T plot showing the first appearance boundaries of most common mineral phases (Pl=plagioclase; Am=amphibole; Mag=magnetite) in water-saturated basaltic andesite (band) and andesite (and) magma buffered at NNO+1 to NNO+2 (from<sup>21</sup>; for simplicity the boundaries of clinopyroxene and olivine have been omitted). Also shown are the solubility curves of a fluid (75 mol.% H<sub>2</sub>O, 25 mol.% CO<sub>2</sub>) in a basaltic magma calculated with VolatileCalc1<sub>1</sub><sup>58</sup>, the projected vapour+liquid coexistence surface for salinities of 10 wt.% and 30–45 wt.% NaCl (green, extrapolated above 1000°C) and the vapour+liquid+halite coexistence curve (blue) from<sup>39</sup> (V=vapour, L=liquid, H=halite, F=single-phase fluid). The orange path 1 represents a hypothetical fluid-unsaturated (e.g., H<sub>2</sub>O=2.5 wt.%) basaltic andesite/andesite magma that ascends rapidly to shallow level until it becomes fluid-saturated upon hitting the 2.5 wt.% H<sub>2</sub>O boundary. This magma will exsolve a fluid below the vapour+liquid coexistence line and will not have significantly high Sr/Y because it will not fractionate amphibole. If the same magma undergoes isobaric crystallization at  $P > \sim 0.2$  GPa (red paths 2) it will eventually become fluid-saturated in the single-phase fluid field, above the vapour+liquid coexistence line. Because amphibole always precedes plagioclase crystallization above the vapour+liquid coexistence line in andesitic magmas and almost at any pressure above the V+L coexistence line for basaltic andesite magmas (except a small gap between  $\sim 0.19$  and  $\sim 0.22$  GPa), it follows that development of high Sr/Y signatures and exsolution of fluids in the single phase field are intimately bound together. Hydrous andesitic magmas rising rapidly to shallow levels have magnetite close to the liquidus (orange path 1), which might cause sulphide saturation before fluid exsolution, depending on the initial water content of the magma. In contrast, andesitic magmas evolving at  $P > 0.2$  GPa and thus acquiring high Sr/Y signatures (red paths 2) will crystallize magnetite late thus making possible the partitioning of Cu into an exsolved fluid before magnetite-induced sulphide saturation incorporates magmatic Cu.

fluid and melt inclusions (which have not been observed in Pilavo rocks) could possibly provide direct evidence for such a process. Our results are consistent with the idea that ore fluids can derive metals directly from mafic-intermediate magmas<sup>26</sup> in addition to remobilizing them from earlier magmatic sulphides<sup>29–31</sup>. Importantly, Cu partitioning into a fluid exsolved from andesitic magma at high-pressure ( $\sim 0.4$  GPa) may provide an explanation for the preferential association of many porphyry-type deposits with high Sr/Y magmas as opposed to low Sr/Y ones.

Pilavo magmas with lower Sr/Y values (40–50) owe their signature to limited amphibole fractionation, which resulted from a short to negligible residence time in a composite mid-crustal reservoir<sup>37</sup>. They have exsolved fluids by decompression at shallow levels, likely below the single-phase fluid field (vapour+liquid; Figure 4). Cu-sulphides trapped in empty inclusions of plagioclases (Figures 2c–f) record the shallow level exsolution from the magma of a Cu-bearing,

mostly vapour-rich fluid. However, vapour exsolution at shallow levels is not considered to be favourable for large porphyry Cu formation<sup>53</sup>. This is due to the fact that vapours are easily dispersed to the atmosphere at these shallow levels and have metal concentrations generally too low to form economic deposits<sup>53</sup>. Large porphyry deposits are usually considered to be formed by a single-phase fluid of variably low salinity exsolved at deeper levels<sup>1,53</sup>.

Magmas at Pilavo, as well as other well-studied magmatic systems associated with porphyry-type deposits (e.g., Yanacocha<sup>8</sup>, Tampakan<sup>7</sup>, porphyry systems in Iran and Pakistan<sup>22</sup>), developed high Sr/Y (>50 and up to 80) signatures through a combination of fractionation, crustal melting and assimilation. All these processes occurred at pressures at which amphibole preceded plagioclase crystallization ( $\sim 0.4$  GPa at Pilavo). In andesite and basaltic andesite magmas amphibole precedes plagioclase fractionation above a pressure threshold ( $\sim 0.2$  GPa), which roughly coincides with the vapour+liquid coexistence lines of low to intermediate salinity fluids (Figure 4). It follows that andesitic magmas that develop high Sr/Y signatures through high-pressure ( $> \sim 0.2$  GPa) crystallization of amphibole will exsolve a single-phase fluid when they reach fluid saturation (Figure 4). Our results show that Cu may efficiently partition into this single-phase fluid exsolved from an andesitic oxidized magma crystallizing at depth, before sulphide saturation.

Fluid saturation in magmas evolving at deep levels, which are therefore likely to develop high Sr/Y signatures, has already been proposed as a solution to the conundrum of excess sulfur released during many volcanic arc eruptions<sup>45</sup>. Our data suggest that oxidized, high Sr/Y magmas formed through mid-crustal fractionation  $\pm$  crustal melting and assimilation likely coexist at depth with an excess fluid containing not only S but also Cu. The evidence of a Cu-bearing excess fluid in the higher Sr/Y andesitic magmas of Pilavo reconciles into a coherent model of porphyry systems: (i) the idea that shallow porphyry systems are fed by Cu-bearing fluids escaping periodically from a deep mafic/intermediate reservoir and/or advected with the magma itself<sup>32,33</sup>, and (ii) the spatial-temporal association of porphyry systems with high Sr/Y magmas (see above). In this model cyclic replenishments of the deep reservoir by mafic recharges may cause cyclic fluid saturation through high-pressure crystallization (see also<sup>7</sup>). By this way fluid and metal flux from the deep mafic-intermediate reservoir may continue for prolonged time because deep reservoirs are more easily kept at mature thermal conditions by recharge processes than shallow ones. This results in a long-lived, continuous fertilization of the shallow magmatic-hydrothermal systems<sup>7,8</sup> and is consistent with the long hydrothermal life of giant porphyry systems (e.g.<sup>54</sup>). During this time, and depending on crustal stress conditions, the high Sr/Y signature may also be episodically transferred to shallower levels by magma pulses ascending from the deep reservoir. This may cause the frequent, but not universal, association of high Sr/Y magmatic rocks with large porphyry systems.

## Methods

In situ trace element analyses of amphibole, clinopyroxene and plagioclase were carried out on polished thin sections by LA-ICP-MS using a Perkin Elmer ELAN 6100 DRX ICP-MS equipped with a 193 nm EXCIMER Geolas laser at the University of Lausanne (Switzerland). Operating conditions of the laser were: 8 Hz frequency, 100 mJ energy, 35 or 60  $\mu$ m spot size. CaO contents determined by microprobe in the area of subsequent ablation with the laser were used for internal standardization by reference to an SRM612 NIST external standard. Raw data were reduced off-line using the LAMTRACE software<sup>55–57</sup>. Element concentrations are reported in Supplementary Material 2. The reproducibility ( $1\sigma$ ) of the measured trace elements in the SRM612 standard is  $< 10\%$ .

SEM imaging and EDS analyses were carried out on a JSM-7001F JEOL scanning electron microscope at the Section of Earth and Environmental Sciences, University of Geneva (Switzerland) on both thin polished sections and hammer-broken, air gun-blown and unwashed rock splits to avoid dissolution of soluble minerals potentially present in fluid inclusions.

1. Sillitoe, R. H. Porphyry copper systems. *Econ. Geol.* **105**, 3–41 (2010).



2. Sillitoe, R. H. A plate tectonic model for the origin of porphyry copper deposits. *Econ. Geol.* **67**, 184–197 (1972).
3. Thieblemont, D., Stein, G. & Lescuyer, J. L. Epithermal and porphyry deposits: the adakite connection. *Comptes Rend. Acad. Sci. Série 2, Sci. Terre Plan.* **325**, 103–109 (1997).
4. Kay, S. M., Mpodozis, C. & Coira, B. Neogene magmatism, tectonism, and mineral deposits of the Central Andes (22° to 33°S latitude). In: Skinner, B. J. (Ed), *Geology and ore deposits of the Central Andes*, SEG Special Publication N. 7, pp. 27–59 (1999).
5. Kay, S. M. & Mpodozis, C. Central Andean ore deposits linked to evolving shallow subduction systems and thickening crust. *GSA Today* **11**, 4–9 (2001).
6. Cooke, D., Hollings, P. & Walshe, J. L. Giant porphyry deposits: characteristics, distribution, and tectonic controls. *Econ. Geol.* **100**, 801–818 (2005).
7. Rohrlach, B. D. & Loucks, R. L. Multi-Million-Year Cyclic Ramp-Up of Volatiles in a Lower Crustal Magma Reservoir Trapped Below the Tappan Cu-Au Deposit by Mio-Pliocene Crustal Compression in the Southern Philippines. In: Porter, T. M. (Ed), *Super Porphyry Copper & Gold Deposits - A Global Perspective*, PGC Publishing, Adelaide, v. 2, pp. 369–407 (2005).
8. Chiaradia, M., Merino, D. & Spikings, R. Rapid transition to long-lived deep crustal magmatic maturation and the formation of giant porphyry-related mineralization (Yanacocha, Peru). *Earth Planet. Sci. Lett.* **288**, 505–515 (2009).
9. Shafiei, B., Haschke, M. & Shahabpour, J. Recycling of orogenic arc crust triggers porphyry Cu mineralization in Kerman Cenozoic arc rocks, southeastern Iran. *Min. Dep.* **44**, 265–283 (2009).
10. Richards, J. P. High Sr/Y arc magmas and porphyry Cu±Mo±Au deposits: just add water. *Econ. Geol.* **106**, 1075–1081 (2011).
11. Defant, M. J. & Drummond, M. S. Derivation of some modern arc magmas by melting of young subducted lithosphere. *Nature* **347**, 662–665 (1990).
12. Martin, H., Smithies, R. H., Rapp, R., Moyen, J.-F. & Champion, D. An overview of adakite, tonalite-trondhjemite-granodiorite (TTG), and sanukitoid: relationships and some implications for crustal evolution. *Lithos* **79**, 1–24 (2005).
13. Petford, N. & Gallagher, K. Partial melting of mafic (amphibolitic) lower crust by periodic influx of basaltic magma. *Earth Planet. Sci. Lett.* **193**, 483–499 (2001).
14. Zellmer, G. F., Iizuka, Y., Miyoshi, M., Tamura, Y. & Tatsumi, Y. Lower crustal H<sub>2</sub>O controls on the formation of adakitic melts. *Geology* **40**, 487–490 (2012).
15. Müntener, O., Kelemen, P. B. & Grove, T. L. The role of H<sub>2</sub>O during crystallization of primitive arc magmas under uppermost mantle conditions and genesis of igneous pyroxenites: an experimental study. *Contrib. Mineral. Petrol.* **141**, 643–658.
16. Alonso-Perez, R., Müntener, O. & Ulmer, P. Igneous garnet and amphibole fractionation in the roots of island arcs: experimental constraints on H<sub>2</sub>O undersaturated andesite liquids. *Contrib. Mineral. Petrol.* **157**, 541–558 (2009).
17. Macpherson, C. G., Dreher, S. T. & Thirlwall, M. F. Adakites without slab melting: high pressure differentiation of island arc magma, Mindanao, The Philippines. *Earth Planet. Sci. Lett.* **243**, 581–593 (2006).
18. Rodríguez, C., Sellés, D., Dungan, M., Langmuir, C. & Leeman, W. Adakitic Dacites Formed by Intracrustal Crystal Fractionation of Water-rich Parent Magmas at Nevado de Longaví Volcano (36°2'S; Andean Southern Volcanic Zone, Central Chile). *J. Pet.* **48**, 2033–2061 (2007).
19. Chiaradia, M. Adakite-like magmas from fractional crystallization and melting-assimilation of mafic lower crust (Eocene Macuchi arc, Western Cordillera, Ecuador). *Chem. Geol.* **265**, 468–487 (2009).
20. Chiaradia, M., Müntener, O., Beate, B. & Fontignie, D. Adakite-like volcanism of Ecuador: lower crust magmatic evolution and recycling. *Contrib. Mineral. Petrol.* **158**, 563–588 (2009).
21. Mungall, J. E. Roasting the mantle: Slab melting and the genesis of major Au and Au-rich Cu deposits. *Geology* **30**, 915–918 (2002).
22. Richards, J. P. & Kerrich, R. Adakite-like rocks: Their diverse origins and questionable role in metallogenesis. *Econ. Geol.* **102**, 537–576 (2007).
23. Richards, J. P., Spell, T., Rameh, E., Raziq, A. & Fletcher, T. High Sr/Y magmas reflect arc maturity, high magmatic water content, and porphyry Cu±Mo±Au potential: examples from the Tethyan arcs of Central and Eastern Iran and Western Pakistan. *Econ. Geol.* **107**, 295–332 (2012).
24. Chambeffort, I., Dilles, J. H. & Kent, A. J. R. Anhydrite-bearing andesite and dacite as a source for sulfur in magmatic-hydrothermal mineral deposits. *Geology* **36**, 719–722 (2008).
25. Lee, C.-T. A., Luffi, P., Chin, E. J., Bouchet, R., Dasgupta, R., Morton, D. M., Le Roux, V., Yin, Q.-Z. & Jin, D. Copper systematics in arc magmas and implications for crust-mantle differentiation. *Science* **336**, 64–68.
26. Cline, J. S. & Bodnar, R. J. Can economic porphyry copper mineralization be generated by a typical calc-alkaline melt? *J. Geophys. Res.* **96**, 8113–8126 (1991).
27. Ulrich, T., Günther, D. G. & Heinrich, C. A. Gold concentrations of magmatic brines and the metal budget of porphyry copper deposits. *Nature* **399**, 676–679 (1999).
28. Zajacz, Z. & Halter, W. Copper transport by high temperature, sulfur-rich magmatic vapor: evidence from silicate melt and vapor inclusions in a basaltic andesite from the Villarica volcano (Chile). *Earth Planet. Sci. Lett.* **282**, 115–121 (2009).
29. Candela, P. A. & Holland, H. D. A mass transfer model for copper and molybdenum in magmatic hydrothermal systems: the origin of porphyry-type deposits. *Econ. Geol.* **81**, 1–19 (1986).
30. Halter, W. E., Heinrich, C. A. & Pettke, T. Magma evolution and the formation of porphyry Cu–Au ore fluids: evidence from silicate and sulfide melt inclusions. *Mineral. Depos.* **39**, 845–863 (2005).
31. Nadeau, O., Williams-Jones, A. E. & Stix, J. Sulphide magma as a source of metals in arc-related magmatic hydrothermal ore fluids. *Nature Geoscience* **3**, 501–505 (2010).
32. Hattori, K. High-sulfur magma, a product of fluid discharge from underlying mafic magma: Evidence from Mount Pinatubo, Philippines. *Geology* **21**, 1083–1086 (1993).
33. Lowenstern, J. B. Dissolved volatile concentrations in an ore-forming magma. *Geology* **22**, 893–896 (1994).
34. Hattori, K. & Keith, J. D. Contribution of mafic melt to porphyry copper mineralization: evidence from Mount Pinatubo, Philippines, and Bingham Canyon, Utah, USA. *Min. Dep.* **26**, 799–806 (2001).
35. Stern, C. R. & Skewes, M. A. Origin of giant Miocene and Pliocene Cu–Mo deposits in Central Chile: role of ridge subduction, decreased subduction angle, subduction erosion, crustal thickening, and long-lived, batholith-size, open-system magma chambers. In: Porter, T. M. (Ed), *Super Porphyry Copper & Gold Deposits - A Global Perspective*, PGC Publishing, Adelaide, v. 1, pp. 65–82 (2005).
36. Stern, C. R., Skewes, M. A. & Arévalo, A. Magmatic Evolution of the Giant El Teniente Cu–Mo Deposit, Central Chile. *J. Pet.* **52**, 1591–1617 (2011).
37. Chiaradia, M., Müntener, O. & Beate, B. Enriched basaltic andesites from mid-crustal fractional crystallization, recharge, and assimilation (Pilavo volcano, Western Cordillera of Ecuador). *J. Pet.* **52**, 1107–1141 (2011).
38. Lange, R. A., Frey, H. M. & Hektor, J. A thermodynamic model for the plagioclase-liquid hygrometer/thermometer. *American Mineralogist* **94**, 494–506 (2009).
39. Candela, P. A. & Holland, H. D. The partitioning of copper and molybdenum between silicate melts and aqueous fluids. *Geochim. Cosmochim. Acta* **4**, 373–380 (1984).
40. Williams, T. J., Candela, P. A. & Piccoli, P. M. The partitioning of copper between silicate melts and two-phase aqueous fluids: An experimental investigation at 1 kbar, 800°C and 0.5 kbar, 850°C. *Contrib. Mineral. Petrol.* **121**, 388–399 (1995).
41. Simon, A. C., Pettke, T., Candela, P. A., Piccoli, P. M. & Heinrich, C. A. Copper partitioning in a melt–vapor–brine–magnetite–pyrrhotite assemblage. *Geochim. Cosmochim. Acta* **70**, 5583–5600 (2006).
42. Jugo, P. J., Candela, P. A. & Piccoli, P. M. Magmatic sulfides and Au:Cu ratios in porphyry deposits: an experimental study of copper and gold partitioning at 850°C, 100 MPa in a haplogranitic melt–pyrrhotite–intermediate solid solution–gold metal assemblage, at gas saturation. *Lithos* **46**, 573–58 (1999).
43. Rowe, M. C., Kent, A. J. R. & Thornber, C. R. Using amphibole phenocrysts to track vapor transfer during magma crystallization and transport: An example from Mount St. Helens, Washington. *J. Volcan. Geotherm. Res.* **178**, 593–607 (2008).
44. Jenner, F. E., O'Neill, H. St. C., Arculus, R. J. & Mavrogenes, J. A. The Magnetite Crisis in the Evolution of Arc-related Magmas and the Initial Concentration of Au, Ag and Cu. *J. Pet.* **51**, 2445–2464 (2010).
45. Wallace, P. J. Volcanic SO<sub>2</sub> emissions and the abundance and distribution of exsolved gas in magma bodies. *J. Volcan. Geotherm. Res.* **108**, 85–106 (2001).
46. Zajacz, Z., Seo, J. H., Candela, P. A., Piccoli, P. M. & Tossell, J. A. The solubility of copper in high-temperature magmatic vapors: a quest for the significance of various chloride and sulfide complexes. *Geochim. Cosmochim. Acta* **75**, 2811–2827 (2011).
47. Berlo, K., Blundy, J., Turner, S., Cashman, K., Hawkesworth, C. & Black, S. Geochemical precursors to volcanic activity at Mount St. Helens, USA. *Science* **306**, 1167–1169 (2004).
48. Audetat, A. & Pettke, T. The magmatic-hydrothermal evolution of two barren granites: a melt and fluid inclusion study of the Rito del Medio and Canada Pinabete plutons in northern New Mexico (USA). *Geochim. Cosmochim. Acta* **67**, 97–121 (2003).
49. Sun, W., Arculus, R. J., Kamenetski, V. S. & Binns, R. A. Release of gold-bearing fluids in convergent margin magmas prompted by magnetite crystallization. *Nature* **431**, 975–978 (2004).
50. Moore, G. & Carmichael, I. S. E. The hydrous phase equilibria (to 3 kbar) of an andesite and basaltic andesite from western Mexico: constraints on water content and conditions of phenocryst growth. *Contrib. Mineral. Petrol.* **130**, 304–319 (1998).
51. Gualda, G. A. R. & Ghiorso, M. S. Magnetite scavenging and the buoyancy of bubbles in magmas. Part 2: Energetics of crystal-bubble attachment in magmas. *Contrib. Mineral. Petrol.* **154**, 479–490 (2007).
52. Richards, J. P. Tectono-Magmatic Precursors for Porphyry Cu–(Mo–Au) Deposit Formation. *Econ. Geol.* **98**, 1515–1533 (2003).
53. Williams-Jones, A. E. & Heinrich, C. A. Vapor transport and the formation of magmatic-hydrothermal ore deposits. *Econ. Geol.* **100**, 1287–1312 (2005).
54. Makshev, V., Munizaga, F., McWilliams, M., Fanning, M., Mathur, R., Ruiz, J. & Zentilli, M. New Chronology for El Teniente, Chilean Andes, from U–Pb, <sup>40</sup>Ar/<sup>39</sup>Ar, Re–Os, and Fission-Track Dating: Implications for the Evolution of a Supergiant Porphyry Cu–Mo Deposit. *SEG Special Publication N. 11*, p. 15–54 (2004).
55. Jackson, S. E., Longrich, H. P., Dunning, G. R. & Fryer, B. J. The application of laser ablation microprobe–inductively coupled plasma–mass spectrometry (LAM–ICP–MS) to in situ trace element determinations in minerals. *Canadian Mineralogist* **30**, 1049–1064 (1992).



56. Jackson, S. LAMTRACE data reduction software for LA-ICP-MS. *Mineralogical Association of Canada Short Course Series* **40**, 305–307 (2008).
57. Longerich, H. P., Jackson, S. E. & Günther, D. Laser ablation–inductively coupled plasma–mass spectrometric transient signal data acquisition and analyte concentration calculation. *J. Anal. Atomic Spectrom.* **11**, 899–904 (1996).
58. Newman, S. & Lowenstern, J. B. VolatileCalc: a silicate melt-H<sub>2</sub>O-CO<sub>2</sub> solution model written in Visual Basic for Excel. *Computers and Geosciences* **28**, 597–604 (2002).
59. Driesner, T. & Heinrich, C. A. The System H<sub>2</sub>O-NaCl. I. Correlations for molar volume, enthalpy, and isobaric heat capacity from 0 to 1000°C, 1 to 5000 bar, and 0 to 1 X<sub>NaCl</sub>. *Geochim. Cosmochim. Acta* **71**, 4902–4919 (2007).

## Acknowledgements

We acknowledge the Swiss National Science Foundation (projects N. 200020-117616 and 200020\_126896 granted to MC) for funding this study. We thank the constructive reviews of Adam Simon, Sue Kay and Keiko Hattori. We are also grateful to Ryan Cochrane for reviewing the English of the manuscript and to Agathe Martignier for the help during SEM imaging.

## Author contributions

MC, AU and KK were involved in designing the study and collecting and analysing the data. BB was involved in collecting the samples and providing the geological background. MC, AU, KK, and BB were involved in the writing and editing. All authors reviewed the manuscript.

## Additional information

**Supplementary information** accompanies this paper at <http://www.nature.com/scientificreports>

**Competing financial interests:** The authors declare no competing financial interests.

**License:** This work is licensed under a Creative Commons

Attribution-NonCommercial-NoDerivative Works 3.0 Unported License. To view a copy of this license, visit <http://creativecommons.org/licenses/by-nc-nd/3.0/>

**How to cite this article:** Chiaradia, M., Ulianov, A., Kouzmanov, K. & Beate, B. Why large porphyry Cu deposits like high Sr/Y magmas? *Sci. Rep.* **2**, 685; DOI:10.1038/srep00685 (2012).